

Electro-Fenton Degradation of High Concentration Rhodamine B on Nickel Foam Cathode Catalyzed by Cucumber Bio-Templated Fe₃O₄@PTFE

Chang Yang¹, Huidong Xie^{2,*}, Zhiteng Wang², Yurong Tan², Na Wang³

¹ Division of Laboratory and Equipment Management, Xi'an University of Architecture and Technology, Xi'an, 710055, Shaanxi, China.

² School of Chemistry and Chemical Engineering, Xi'an University of Architecture and Technology, Xi'an, 710054, Shaanxi, China.

³ College of Architecture and Civil Engineering, Xi'an University of Science and Technology, Xi'an, 710054, Shaanxi, China.

*E-mail: xiehuidong@tsinghua.org.cn

Received: 21 September 2020 / Accepted: 14 November 2020 / Published: 30 November 2020

Electro-Fenton technology has a great advantage in the treatment of high concentration refractory organic wastewater. In this paper, nickel foam was used as the cathode and cucumber bio-templated Fe₃O₄ was used as the catalyst to degrade rhodamine B by the electro-Fenton method. The active species in the degradation process were studied, and the degradation conditions were optimized. The results showed, compared with analytical reagent Fe₃O₄, the as-prepared cucumber bio-templated Fe₃O₄ has a larger specific surface area, a greater degradation efficiency, a higher concentration of generated •OH, and a lower concentration of generated H₂O₂. Hydroxyl radical is the active species during the electro-Fenton degradation. The degradation efficiency of 100 mg/L rhodamine B catalyzed by cucumber bio-templated Fe₃O₄ can reach 81.8% under the conditions of pH 3 and a current of 10 mA.

Keywords: electro-Fenton; Fe₃O₄; nickel foam; Rhodamine B; bio-templated.

1. INTRODUCTION

At present, water pollution has caused serious damage to the environment and human health. Compared with the photocatalytic method reported in the literature[1], homogeneous Fenton or electro-Fenton oxidation technology has shown greater advantages in the treatment of dye wastewater with high concentration [2,3]. Moreira et al. [4] reported that the Fenton-like method can treat the wastewater with dye concentration in the range of 1.4~3580 mg/L, which was much higher than that of 5~10 mg/L commonly used in photocatalytic degradation. As well known, cathode materials play an important role

to improve the pollutant degradation efficiency in the electro-Fenton system. Foam metal is conductive and has a large surface area, which is beneficial for the generation of H_2O_2 when used as a cathode in the electro-Fenton technology. Liu et al. [5,6] reported a three-dimensional electro-Fenton system using nickel foam as cathode for the treatment of rhodamine B solution, whose results showed the degradation efficiency of rhodamine B was 99% under neutral conditions for 30 min. For an electro-Fenton method, various iron oxides, such as goethite (FeOOH), magnetite (Fe_3O_4), and hematite (Fe_2O_3)[7,8], are often used as catalysts for the production of $\cdot\text{OH}$. Among them, Fe_3O_4 is widely studied because it has Fe(II) to catalyze Fenton reaction as well as magnetic properties which make it easy to separate, recover, and recycle. He et al. [9] used magnetic nano- Fe_3O_4 particles as the catalyst to degrade C.I reactive blue 19, whose removal efficiency of total organic carbon (TOC) reached 87% at $\text{pH} = 3$ for 120 min. Nguyen et al. [10] prepared Zn doped Fe_3O_4 hollow microspheres and utilized these microspheres for the degradation of rhodamine B and cefalexin by visible light Fenton method. They noticed that 97% of rhodamine B and 90% of cefalexin were removed in 60 min and 180 min, respectively. For the catalyst preparation methods, many studies focus on using natural bio-materials as templates to prepare micro- or nano- three-dimensional porous structures[11]. Yu et al. [12] prepared carbon-doped TiO_2 using corn stalk as a template, and the removal efficiency of total carbon (TC) reached 100% in 40 min under ultraviolet assisted Fenton-like condition. However, the preparation of Fe_3O_4 by the biological templated method and its application as an electro-Fenton catalytic material have not been reported in the literature.

In the current work, porous Fe_3O_4 materials with large surface area and high porosity were obtained through an impregnation and calcination method with porous cucumber as a template. The bio-templated Fe_3O_4 was loaded on the nickel foam cathode and employed for the degradation of rhodamine B by the electro-Fenton process. The degradation conditions of rhodamine B were optimized and the degradation mechanism of rhodamine B was discussed.

2. EXPERIMENTAL

2.1 Reagents and instruments

The pore size, porosity, and thickness of the nickel foam were 230 μm , 98%, and 1 mm, respectively. Other reagents were analytical reagents (A.R.). Polytetrafluoroethylene (PTFE) powder was purchased from Chongqing Songbai Chemical Plant. Fe_3O_4 was purchased from Tianjin Fuchen Chemical Reagent Plant.

The X-ray diffraction pattern was measured on a Bruker D8 advance diffractometer with a Cu K_α radiation. The morphology and energy dispersive spectra were analyzed by an FEI Quanta F250 scanning electron microscope. The specific surface area and pore size of the samples were measured by a JW-BK300C nitrogen adsorption-desorption instrument at 77K. The samples were pretreated at 523K for 12 hours to remove the adsorbed impurity gas before the measurement.

2.2 Preparation of nickel foam electrode loaded with cucumber-templated Fe_3O_4 and measurement of the H_2O_2 yield

First, cucumber was cut into slices and impregnated in nitric acid solution at pH 3 for 0.5 h, and then the excess acid was removed by rinsing with deionized water. Subsequently the pretreated cucumber was added into 400 ml 50% ethanol solution and soaked for 24 h. After that, the cucumber slices were filtered out and dried. Then the as-pretreated slices were immersed in a 0.25 mol/L FeSO_4 solution, which was placed in a thermostatical water bath oscillator (temperature: 30°C, rotary speed: 160 r/min). After shaking for 12 h, the loaded cucumber was taken out, washed, dried in an oven at 45°C, and ground into powders. Finally, the cucumber-templated Fe_3O_4 was obtained by calcining the powders at 550°C for 2 hours in N_2 atmosphere.

A nickel foam of $2 \times 6 \text{ cm}^2$ was cut and cleaned with ethanol, acetone and deionized water for 30 min, sequentially and then dried. The cucumber-templated Fe_3O_4 and polytetrafluoroethylene powder (PTFE) with a weight ratio of 2:1 were ground in an agate mortar with 4 mL anhydrous ethanol. The ground paste was pasted on the pretreated nickel foam and dried at room temperature. Finally, the cucumber-templated Fe_3O_4 @PTFE electrode was made with further calcination of the pasted nickel foam at 300°C for 1 h. PTFE pasted on the pretreated nickel foam was used as blank. For comparison, A.R. Fe_3O_4 was used to replace the cucumber-templated Fe_3O_4 .

The concentration of H_2O_2 was determined by an iodine reagent method. One milliliter iodine reagent and 1.00 mL 0.10 mol/L potassium hydrogen phthalate were added into 200ml solution. The absorbance at 352 nm of the solution was measured by a UV-Vis spectrophotometer to determine the H_2O_2 concentration.

2.3 Degradation of rhodamine B dye and determination of $\bullet\text{OH}$

The experimental schematic diagram is shown in Fig. 1. The electro-Fenton system without membrane was composed of a $2 \times 6 \text{ cm}^2$ graphite sheet as the anode, a cucumber-templated Fe_3O_4 @PTFE electrode as the cathode, 0.05 mol/L Na_2SO_4 as the supporting electrolyte, and a 300 mL quartz beaker as the reaction vessel. One hundred mg/L rhodamine B was degraded in the vessel.

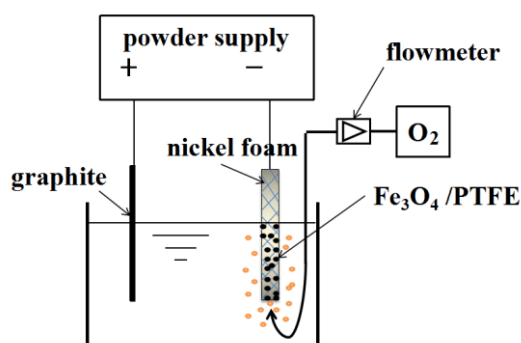


Figure 1. Schematic diagram of the experimental device.

The constant current was provided and controlled by a potentiostat (DJS-292, Shanghai Leicichuangyi Instrument Co., Ltd.). The pH of the solution was adjusted, and oxygen was continuously introduced under the cathode in the electrolysis process to generate H₂O₂. Every 8 minutes 2.00 ml solution was taken, centrifuged, and diluted for the measurement of the absorbance at 554 nm by a UV-Vis spectrophotometer.

The removal efficiency of rhodamine B was calculated by the formula (1) as follows:

$$\eta = \frac{A_0 - A_t}{A_0} \times 100\% \quad (1)$$

where A_0 and A_t are the absorbances of rhodamine B after adsorption equilibrium and after electro-Fenton degradation for a certain time.

For the reusability tests of cathodic materials, the cucumber-templated Fe₃O₄@PTFE electrode was repeatedly cleaned with deionized water and dried in the air after the previous experiment. The experimental conditions were same to the optimal condition: initial concentration rhodamine B of 100 mg/L, current of 10 mA, pH of 3, and supply of oxygen. The composite electrode was reused for 3 times.

The fluorescence intensity method of coumarin was used to detect the •OH concentration produced in the degradation process. First 0.2023 g coumarin was weighed and added to the above degradation solution. Then 2.00 ml solution was transferred with a pipette gun and diluted for the measurement of fluorescence intensity at 322 nm or 454 nm.

3. RESULTS AND DISCUSSION

3.1 Characterization of cucumber-templated Fe₃O₄

Fig. 2(a) shows the XRD patterns of cucumber-templated Fe₃O₄. The XRD pattern is consistent with the standard card of Fe₃O₄ (JCPDS No: 75-0033). Fig. 2(b) shows the nitrogen adsorption-desorption isotherm curves of A.R. and cucumber-templated Fe₃O₄. As can be seen, in the low-pressure area ($P/P_0 = 0 \sim 0.1$), the adsorption line of cucumber-templated Fe₃O₄ is more inclined to the Y-axis which belongs to type IV, indicating that the material has a strong force with N₂. In the medium pressure area ($P/P_0 = 0.3 \sim 0.8$), the adsorption curve does not coincide with the desorption curve with an obvious hysteresis loop which is consistent with type H3. The above results show that the cucumber-templated Fe₃O₄ is a mesoporous (2~50 nm) material with a large specific surface area and abundant active sites and the pore is composed of the slit with particle accumulation. The calculated specific surface area, pore volume and average pore diameter of particles are compared and listed in Table 1. Fig. 2(c) and Fig. 2(d) are SEM images and EDS results of cucumber-templated Fe₃O₄. As can be seen from Fig. 2(c), cucumber-templated Fe₃O₄ has a loose channel and the particles are close to cubic shape with the size of about 50~200 nm. The EDS result shows that cucumber-templated Fe₃O₄ contains Fe, O, and S elements and the atomic ratio of Fe: O is 1.14: 1. The source of the S element may be caused by a small amount of uncleaned FeSO₄ in the sample.

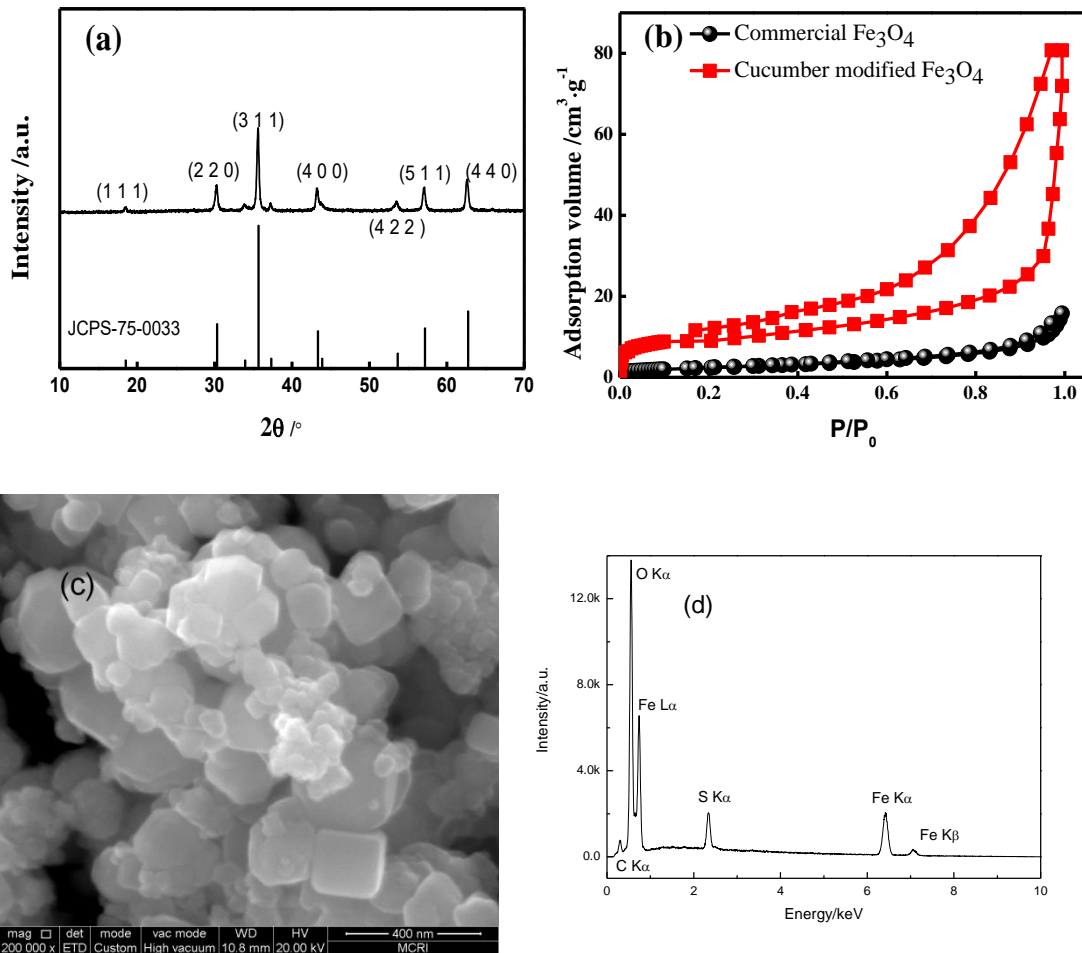


Figure 2. (a) XRD patterns, (b) N_2 adsorption-desorption isotherm curves, (c) Secondary electron image, (d) Energy dispersive spectra of cucumber-templated Fe_3O_4 .

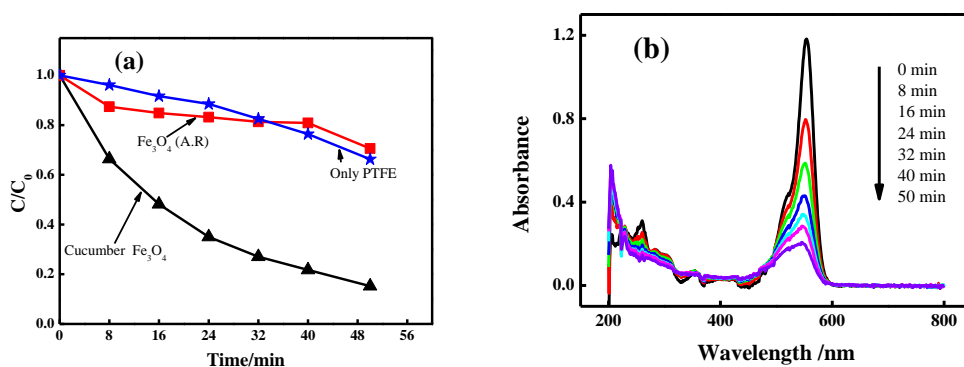
Table 1. Comparison of surface area, pore volume and size between cucumber-templated Fe_3O_4 and A.R. Fe_3O_4

Sample	Surface area (m^2/g)	Pore volume (cm^3/g)	Average pore size (nm)
A.R. Fe_3O_4	8.450	0.02516	10.013
cucumber-templated Fe_3O_4	36.201	0.12567	13.456

3.2 Degradation results and mechanism of rhodamine B

Fig. 3(a) shows the comparison of the degradation result of rhodamine B by PTFE electrode, A.R. $Fe_3O_4@PTFE$ electrode, and cucumber-templated $Fe_3O_4@PTFE$ electrode. In the presence of only PTFE, the degradation efficiency of rhodamine B can reach 29.4% in 50 min, which cannot be ignored. This is because PTFE has suitable permeability and hydrophobicity. When PTFE is added to the electrode, not only the adhesion between the material and the electrode can be improved, but also the

hydrophobicity of the electrode can be enhanced. Hence the adsorption of oxygen on the electrode surface increased, the diffusion of oxygen improved, and the yield of the hydrogen peroxide increased. When using cucumber-templated $\text{Fe}_3\text{O}_4@$ PTFE electrode to degrade rhodamine B, the degradation efficiency of dye can reach a maximum of 81.8% in 50 min. As a contrast, the degradation efficiency of the A.R. $\text{Fe}_3\text{O}_4@$ PTFE electrode is only 27.3% in 50 min. The results also show that the cucumber-templated Fe_3O_4 can more effectively improve the surface area of the catalyst, the reactive sites, and the degradation efficiency of dye than A.R. Fe_3O_4 . The color removal in this work is very close to that in the literature (89.9~98.49%) [13-16]. Fig. 3(b) shows the relationship between absorption spectra of rhodamine B degraded by cucumber-templated Fe_3O_4 and time. As can be seen, the maximum absorption characteristic peak of rhodamine B at 554 nm decreases with the increase of reaction time. This is consistent with the fact that the gradual decolorization of rhodamine B from rose-bengal to colorless. The absorption bands at 353, 303, 259 nm attributed to the π - π^* transitions in aromatic moieties [17] also decrease over time, indicating the destruction of the oxaanthracene and benzene ring in rhodamine B. Fig. 3(c) and 3(d) are time-dependent fluorescent intensity contrast and fluorescent emission spectra of 7-hydroxycoumarin produced by the reaction of $\bullet\text{OH}$ in the solution and coumarin, respectively. The fluorescent intensity of 7-hydroxycoumarin produced by cucumber-templated Fe_3O_4 is the strongest, indicating the greatest concentration of $\bullet\text{OH}$ yield. Considering the degradation efficiency of rhodamine B, it can be concluded that $\bullet\text{OH}$ is the active species to degrade rhodamine B. Fig. 3(e) is the comparison of the H_2O_2 concentration produced by different electrodes. The production of H_2O_2 catalyzed by cucumber-templated Fe_3O_4 is the lowest, indicating that H_2O_2 is not an active species in the process of electro-Fenton degradation. Fig. 3(f) shows the schematic degradation mechanism of rhodamine B by the cathodic electro-Fenton method. Firstly, the introduced O_2 reacts with H^+ in the solution to generate H_2O_2 on the cathode surface, and then H_2O_2 reacts with Fe^{2+} released by Fe_3O_4 loaded on the cathode surface in the acidic environment to generate $\bullet\text{OH}$ [18,19]. The $\bullet\text{OH}$ radical is the second strongest oxidant after fluorine [16,19] which can oxidize and decolorize rhodamine B. As reported by Tian et al.[16], rhodamine B was finally mineralized to CO_2 , H_2O , and salts by $\bullet\text{OH}$ radical in the electro-Fenton process.



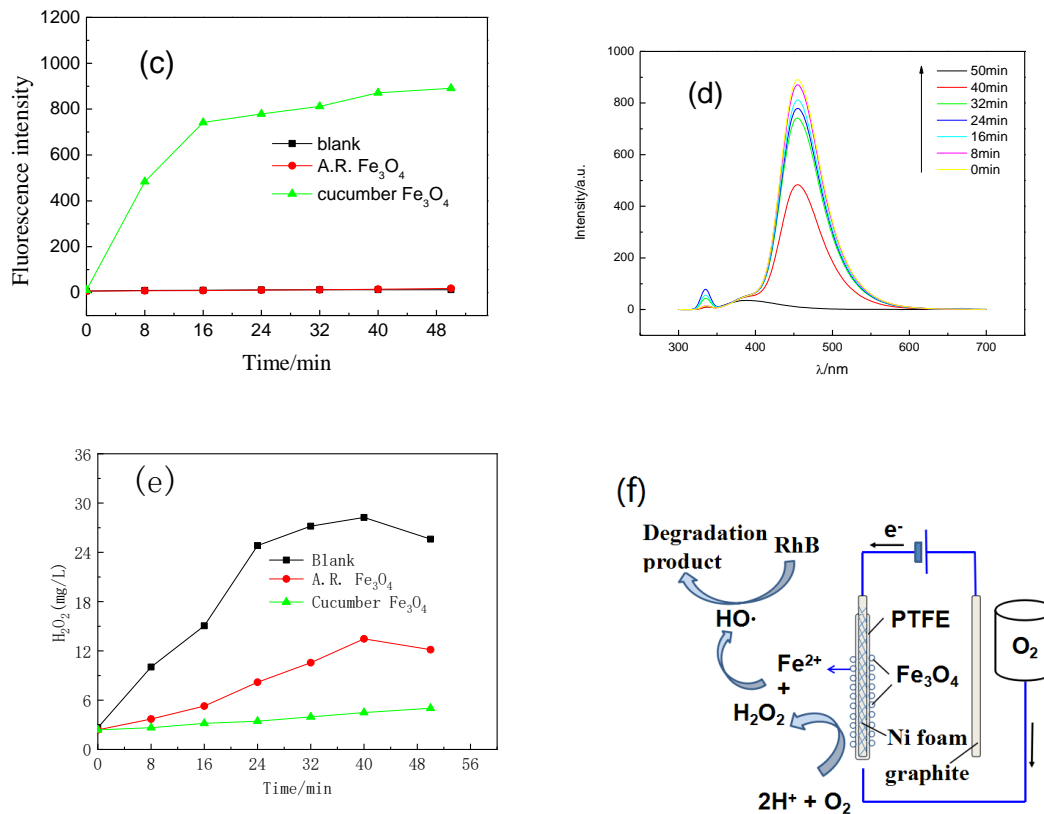


Figure 3. (a) Comparison of the degradation efficiency of rhodamine B by different electrodes vs. time; (b) Time-dependent absorption spectra of rhodamine B degraded by cucumber-templated Fe₃O₄; (c) Comparison of fluorescent intensity of 7-hydroxycoumarin vs. time; (d) Time-dependent fluorescent spectra of 7-hydroxycoumarin of cucumber-templated Fe₃O₄; (e) Comparison of H₂O₂ concentration by different electrodes vs. time; (f) Schematic degradation mechanism of rhodamine B degraded by electro-Fenton.

3.3 Effects of experimental conditions on degradation efficiency of rhodamine B

Fig. 4 shows the effect of different experimental conditions on the degradation efficiency of rhodamine B. From Fig. 4(a), the pH of the solution has a great influence on the degradation efficiency of rhodamine B. At pH = 3, the degradation efficiency of rhodamine B reached the maximum of 81.8% for 50 min. With the increase in pH, the degradation efficiency of rhodamine B decreased gradually. The reason may be that the high concentration of H⁺ at pH 3 can react with the oxygen in the solution to generate more H₂O₂, which is beneficial for the production of •OH and the degradation [20,21]. With the increase in pH, the concentration of H⁺ decreased, which will reduce the production rate of H₂O₂. On the other hand, free Fe²⁺ will gradually reduce with the increase in pH due to the formation of insoluble complexes [22]. From Fig. 4(b), the degradation efficiency of rhodamine B by pure oxygen is greater than that of agitation, and the degradation efficiency of rhodamine B by agitation is greater than that of air pump oxygen supply, indicating that sufficient oxygen dissolution and diffusion in the solution can accelerate the generation of H₂O₂ and •OH and facilitate the degradation reaction. Fig. 4(c) shows a comparison of the effect of current on the degradation efficiency of rhodamine B. When the current is 5

mA, 10 mA and 15 mA, the degradation efficiency of rhodamine B is 49.6%, 81.8% and 72.2%, respectively. Thus, the optimal current value is 10 mA. Too high or too low current density is not beneficial for the reaction [23]. Fig. 4(d) shows the degradation efficiency of different rhodamine B concentrations vs. time. The lower the rhodamine B concentration, the higher the degradation efficiency. The degradation efficiency of 50 mg/L rhodamine B can reach 98.25% for 50 min. When the dye concentration is low, the generated $\bullet\text{OH}$ in the system can effectively react with the chromophore on the dye and attack the electron-rich group of rhodamine B, so the degradation products can be removed quickly. The increase of pollutant concentration will occupy more active sites [24], and only a small amount of $\text{Fe}^{2+}/\text{Fe}^{3+}$ active sites are used for H_2O_2 decomposition, so the content of $\bullet\text{OH}$ in the system decreases.

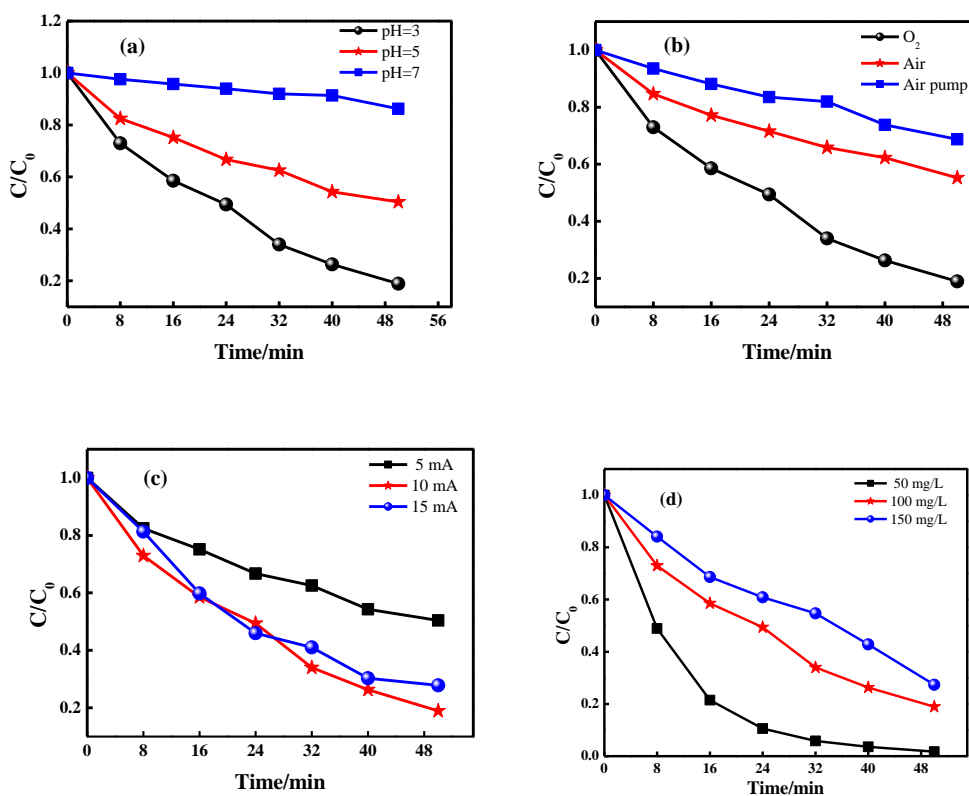


Figure 4. (a) Effect of pH on the degradation of rhodamine B vs. time; (b) Effect of oxygen supply on the degradation of rhodamine B vs. time; (c) Effect of current on the degradation of rhodamine B vs. time; (d) Effect of dye concentration on the degradation of rhodamine B vs. time.

3.4 Recycling tests of cathodic materials

The recyclability and stability of electrodes are very important for the application of the degradation. Fig. 5 shows the effect of recycling times on the degradation of rhodamine B. As shown in the figure, when the fourth degradation experiment was carried out, the degradation efficiency was reduced to 21.7%, which was only one fourth of the initial test. The reasons might be due to two aspects: (1) the electrode material is easy to be polluted in high concentration rhodamine B solution, which makes

the decolorization active site inactivated [17]; (2) nickel foam is unstable and easy to be corroded in acidic solution.

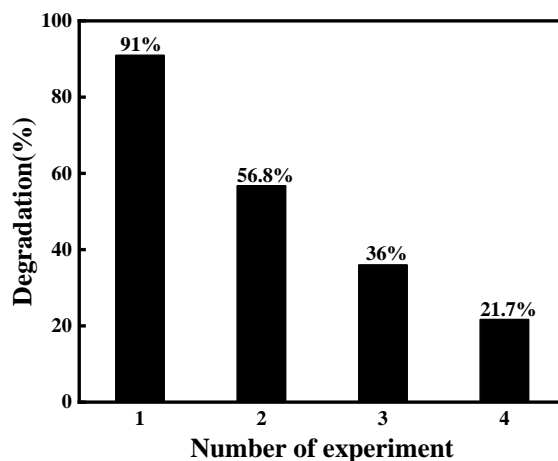


Figure 5. RhB degradation in 4 recycling tests of cathodic materials.

4. CONCLUSION

Cucumber-templated Fe_3O_4 was prepared by the immersion method with the acid treated cucumber as the template. The as-prepared cucumber-templated Fe_3O_4 is a single-phase nanostructured material with a large specific surface area and rich catalytic active sites. Compared with the A.R. Fe_3O_4 , the degradation efficiency of rhodamine B on the composite electrode with the cucumber-templated Fe_3O_4 as catalyst was higher. Under the condition of pH 3 and the current of 10 mA, the degradation efficiency of 100 mg/L rhodamine B could reach 81.8% for 50 min. However the stability and reusability of the cucumber-templated Fe_3O_4 @PTFE electrode need to be improved. Hydroxyl radical ($\bullet\text{OH}$) is the active species in the degradation of rhodamine B.

ACKNOWLEDGEMENT

The research was supported by the National Science Foundation of China under grant no. 51708447 and Key R & D Program of Shaanxi Province under grant no. 2019SF-250.

References

1. H. Tong, S. X. Ouyang, Y.P. Bi, N. Umezawa, M. Oshikiri, and J.H. Ye, *Adv. Mater.*, 24 (2012) 229.
2. E. Brillas, I. Sirés, and M.A. Oturan, *Chem. Rev.*, 109 (2009) 657.
3. I. Salmerón, K.V. Plakas, I. Sirés, I. Oller, M.I. Maldonado, A.J. Karabelas, and S. Malato, *Appl. Catal. B: Environ.*, 242 (2019) 327.

4. F.C. Moreira, R.A.R. Boaventura, E.Brillas, and V.J.P. Vilar, *Appl. Catal. B: Environ.*, 202 (2017) 217.
5. W. Liu, Z.H. Ai, and L.Z. Zhang, *J. Hazard. Mater.*, 243 (2012) 257.
6. W.B. Wan, Y. Zhang, R. Ji, B.B. Wang, and F. He, *ACS Omega*, 2 (2017) 6104.
7. L.Q. Guo, F. Chen, X.Q. Fan, W.D. Cai, and J.L. Zhang, *Appl. Catal. B: Environ.*, 96 (2010) 162.
8. J.B. Zhang, J. Zhuang, L.Z. Gao, Y. Zhang, N. Gu, J. Feng, D.L. Yang, J.D. Zhu, and X.Y. Yan, *Chemosphere*, 73 (2008) 1524.
9. Z.Q. He, C. Gao, and M.Q. Qian, *Ind. Eng. Chem. Res.*, 53 (2014) 3435.
10. X.S. Nguyen, G.K. Zhang, and X.F. Yang, *ACS Appl. Mater. Interf.*, 9 (2017) 8900.
11. K. Zhang, J.C. Qian, Z.G. Chen, and Q. Wei, *Mater. Rev.*, 30 (2016) 39.(in Chinese)
12. X.D. Yu, X.C. Lin, W. Feng, and W.G. Li, *Appl. Surf. Sci.*, 465 (2019) 223.
13. B.G. Zhang, Y.P. Hou, Z.B. Yu, Y.X. Liu, J. Huang, L. Qian, and J.H. Xiong, *Sep. Purif. Technol.* 210 (2019) 60.
14. Y. Zhang, G.T. Luo, Q. Wang, Y.Q. Zhang, and M.H. Zhou, *Chemosphere* 240 (2020) 124929.
15. R. Jinisha, R. Gandhimathi, S.T. Ramesh, P.V. Nidheesh, and S. Velmathi, *Chemosphere* 200 (2018) 446.
16. J.N. Tian, A.M. Olajuyin, T.Z. Mu, M.H. Yang, and J.M. Xing, *Environ. Sci. Pollut. Res.* 23 (2016) 11574.
17. A. Baddouh, G.G. Bessegato, M.M. Rguiti, B. E. Ibrahimi, L. Bazzi, M. Hilali, and M.V.B. Zanoni, *J. Environ. Chem. Eng.* 6 (2018) 2041.
18. A. Cruz-Rizo, S. Gutiérrez-Granados, R. Salazar, and J.M. Peralta-Hernández, *Sep. Purif. Technol.* 172 (2017) 296.
19. O. García-Rodríguez, JA. Bañuelos, A. El-Ghenymy, L.A. Godínez, E. Brillas, and F.J. Rodríguez-Valadez, *J. Electroanal. Chem.* 767 (2016) 40.
20. I. Sirés, J.A. Garrido, R.M. Rodríguez, E. Brillas, N. Oturan, and M.A. Oturan, *Appl. Catal. B: Environ.*, 72 (2007) 382.
21. N. Masomboon, C. Ratanatamskul, and M.C. Lu, *J. Hazard. Mater.*, 176 (2010) 92.
22. W.A. Simon, E. Sturm, H.J. Hartmann, and U. Weser, *Biochem. Pharmacol.*, 71 (2006) 1337.
23. J.N. Tian, J.X. Zhao, A.M. Olajuyin, M.M. Sharshar, T.Z. Mu, M.H. Yang, and J.M. Xing, *Environ. Sci. Pollut. R.*, 23 (2016) 15471.
24. G.H. Zhao, J.X. Gao, W. Shi, M.C. Liu, and D.M. Li, *Chemosphere*, 77 (2009) 188.

© 2021 The Authors. Published by ESG (www.electrochemsci.org). This article is an open access article distributed under the terms and conditions of the Creative Commons Attribution license (<http://creativecommons.org/licenses/by/4.0/>).